

## Effects of the Confined Synthesis on Conjugated Polymer Transport Properties

J. L. Duvail,\* P. Rétho, V. Fernandez, G. Louarn, P. Molinié, and O. Chauvet

*Institut des Matériaux Jean Rouxel, 2 rue de la Houssinière, 44322 Nantes Cedex 3, France*

*Received: July 16, 2004; In Final Form: September 3, 2004*

Previous studies on conjugated polymer nanotubules, prepared by the template method, established that improvements in the molecular and supermolecular structure are responsible for the increase in the room temperature conductivity when the diameter decreases. Our study clearly indicates that a more complex situation can result from the confined synthesis of conjugated polymers in nanopores of a template. Nanowires of poly(3,4-ethylenedioxythiophene), a polythiophene derivative, have been prepared by electrochemical synthesis in polycarbonate templates with diameters ranging between 35 and 200 nm. The electrical transport study (down to 1.5 K) shows that the smaller the nanowire diameter, the stronger the insulating behavior. The temperature dependence of the sample resistance ranges between two extremes, a nonthermally activated regime for the PEDOT film close to the metal–insulator transition and a 2D Mott-variable range hopping-like regime for 35-nm nanowires. It is partly related to the doping level, deduced from X-ray photoelectron spectroscopy (XPS) measurements, which is reduced by about a factor of 2 for 35-nm nanowires, in comparison with the film. But this reduced doping level cannot account for the whole electrical effect. Another important result is the evidence of a decrease in the spin/charge ratio when the nanowire diameter goes from 100 to 50 nm as shown by electron spin resonance (ESR). It suggests that the polaron/bipolaron population ratio is modified. This result will also have important consequences for the transport mechanism.

### Introduction

Properties of nanowires and nanotubes made of conjugated polymers (CP) are much investigated at present for both fundamental and applied reasons. Molecular and supermolecular modifications induced by the synthesis of conjugated polymers at a submicroscopic scale may result in properties very different from that of the bulk material. The resulting nanomaterials are promising as support for bio- and chemical sensors,<sup>1</sup> field emission displays,<sup>2</sup> nanodevices such as single electron tunneling devices,<sup>3</sup> and nanoLEDs.<sup>4</sup> It is thus crucial to understand and to control the mechanisms responsible for their modified properties in comparison to the bulk materials. Among them, electrical properties are of importance because many applications are based on the electrical behavior. The electrical conductance of conjugated polymers depends strongly on the doping level and the molecular and supermolecular structure, all parameters which can be drastically modified by the method of synthesis.

Different top-down or bottom-up approaches have been used to synthesize conducting polymer nanostructures. A popular one is the template synthesis, which was broadly developed by Martin's group,<sup>5,6</sup> and which consists of filling the pores of a porous host in a chemical or electrochemical way. Most of the studies on template-grown CP nanowires report on polypyrrole (PPY) and polyaniline (PANI) nanotubes.<sup>7–11</sup> The thiophene family member PEDOT (poly(3,4-ethylenedioxythiophene)) is also widely investigated. This conjugated polymer is already used in many applications (antistatic, anticorrosion, ...) as a hole injector in OLEDs<sup>12</sup> or in plastic memory<sup>13</sup> because of its long period stability in the p-doped state<sup>14</sup> as well as its efficiency in hole injection. PEDOT nanowires have been grown.<sup>15–17</sup> Granström et al. found that the conductivity in the p-doped state

increases when the pore diameter decreases. This improvement of the conducting properties is attributed to an enhancement of the crystallinity as deduced from XRD studies. An enhanced charge delocalization is invoked as well, based on resonant Raman scattering studies.<sup>17</sup>

In this study, PEDOT nanowires with well-controlled diameters ranging between 35 and 200 nm are electrochemically synthesized within the pores of polycarbonate track-etched templates. The lab-scale membranes are very well defined,<sup>18</sup> which give us the opportunity to address accurately the diameter dependence on the transport properties. In contrast with the results generally reported on PPY and PANI nanotubes,<sup>6–9,11</sup> the estimated room temperature conductivity of PEDOT nanowires seems to be only weakly dependent on the nanowire diameter. Electrical transport measurements have been performed down to 1.5 K for nanowires and film. Surprisingly, a reinforcement of the insulating character is evidenced when the diameter decreases. A structural improvement and an increase in the conjugation length for the smaller diameters is usually invoked for other conjugated polymer nanowires, which should result in the opposite behavior. Instead, our results clearly suggest that a competitive effect induced by the confined synthesis is involved. We show that the doping level decreases with the nanowire diameter, as addressed by XPS. We evidence also a decrease in the spin/charge ratio by ESR study when the nanowire diameter goes from 100 to 50 nm. We discuss these results in relation to the transport properties.

### Experimental Section

The PEDOT nanowires were synthesized by confined electropolymerization at a fixed potential of 0.80V versus saturated calomel electrode (SCE) inside nanoporous polycarbonate (PC) membranes. We mainly used track-etched membranes prepared at the Université Catholique de Louvain. They are 20  $\mu\text{m}$  thick

\* Address correspondence to this author. Phone: 00-2-40-37-39-90. Fax: 00-2-40-37-39-91. E-mail: duvail@cnsr-immn.fr.

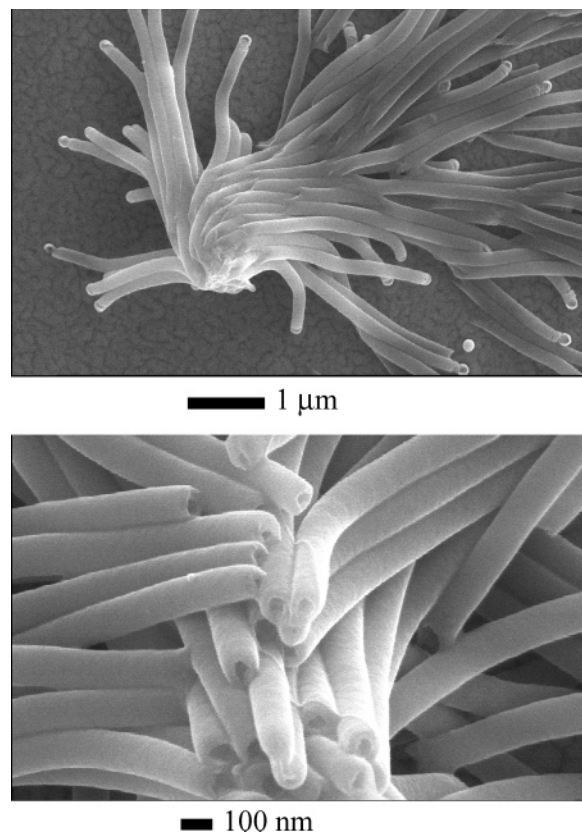


**Figure 1.** SEM images of 150-nm PEDOT nanowires after polycarbonate template removal.

with improved features in comparison to the commercial ones.<sup>18</sup> The diameter distribution relative to the nominal diameter is very narrow and the roughness of the pore surface is very weak. The corresponding pore densities are  $4 \times 10^9$ ,  $1.5 \times 10^9$ , and  $10^8 \text{ cm}^{-2}$  for pore diameters of 35, 75, and 150 nm, respectively. Some PEDOT nanowires were also prepared with commercial PC membranes. These membranes have pores with a cigar-like shape and a rough pore surface. The thickness is about  $10 \mu\text{m}$  and the pore density  $3 \times 10^8 \text{ cm}^{-2}$  for an average pore diameter measured by SEM equal to approximately 200 and 100 nm. For the 50 nm pore diameter, the thickness is about  $6 \mu\text{m}$  and the pore density  $6 \times 10^8 \text{ cm}^{-2}$ . We used a gold layer evaporated on one side of the membrane as the working electrode, a platinum plate as a counter electrode, and a saturated calomel electrode (SCE) as a reference. The polymerization bath consisted of an aqueous solution containing 0.07 M sodium dodecyl sulfate (SDS), 0.1 M  $\text{LiClO}_4$ , and 0.05 M EDOT (monomer distilled before using).<sup>19,20</sup> Field-effect scanning electron microscope (FE-SEM, JEOL 6400 F) images of the nanowires after the PC dissolution with a flow of dichloromethane are shown in Figure 1. The nanowires still attached to the gold layer at the bottom tend to cluster in bundles. The PEDOT nanowires are mainly full cylinders whatever the diameter despite a tubular shape at the top end as previously reported,<sup>17</sup> and in contrast with PPY and PANI nanotubes. A  $6 \mu\text{m}$  thick PEDOT film was prepared on a platinum electrode at the same potential of 0.80 V vs SCE for the sake of comparison. X-ray photoelectron (XPS) spectra were carried out with a vacuum generator KRATOS spectrometer equipped with an Al  $K\alpha$  (1486.6 eV) source operating at 200 W. Low-intensity X-rays were focused on an area of about  $10^4 \mu\text{m}^2$ . The calibration of the XPS spectra was performed by taking the C (1s) electron peak. The electron spin resonance (ESR) study

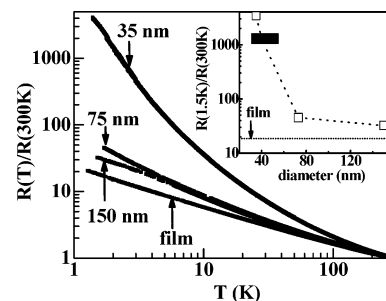


**Figure 2.** Temperature dependence of the resistance  $R(T)$  normalized by  $R(300\text{K})$  for PEDOT nanowires and film. Values (in nanometers) indicate the diameter of the nanowires. Inset:  $\rho_r$  ratio versus the nanowire diameter.

was carried out in a Bruker Elexys spectrometer operating at 9.4 GHz at room temperature. It was checked that saturation or overmodulation did not occur. Electrical measurements in the ohmic regime were obtained in an Oxford Helium gas flow cryostat from 1.5 to 300 K. The film resistance was measured in a four probe configuration with gold evaporated electrodes. A two-probe configuration was used for the nanowires.

## Results

**Transport Measurements.** The DC resistance of nanowires still embedded in the PC membranes were measured by a two-probe method with contacts on both sides of the membrane. The measured resistance is thus the sum of the resistance of hundreds of nearly identical nanowires in parallel and the contact resistance. We took advantages of the very high aspect ratio of the nanowires (up to 500 for a nanowire length of  $20 \mu\text{m}$ ) and the controlled porosity of the lab-scale track-etched membranes (a few percent) to minimize the role of the contact resistance, as mentioned elsewhere.<sup>9,17</sup>

We tried to estimate the room temperature conductivity of these nanowires, assuming that the contacts play a negligible role. It is not possible to give precise values, since the number of connected nanowires is not exactly known. However, a rough estimation of this number gave conductivities of the PEDOT nanowires of the same magnitude as for the PEDOT film ( $61 \text{ S}\cdot\text{cm}^{-1}$ ), whatever the diameter. This result contrasts with the case of PPY and PANI nanotubes, for which a strong increase in the conductivity by a factor 100 is estimated when the diameter decreases from 150 nm to typically 30 nm.<sup>8,9,11</sup> However, Mativetsky and Datars<sup>21</sup> reported recently that the conductivity decreases slightly with the diameter for PPY nanowires prepared by chemical polymerization in commercial polycarbonate templates. This point is discussed later in view of all the results.

The temperature dependence of the resistance  $R(T)/R(300\text{K})$  of the PEDOT nanowires is reported in Figure 2 between 1.5 and 300 K. It gives evidence on the nonmetallic character of the PEDOT. Only small differences in the temperature dependence are observed between the film and the nanowires with diameters down to 75 nm, while a strong increase in the resistance ratio takes place for the 35-nm nanowires at low temperature. It is reflected by the evolution of the corresponding resistance ratio  $\rho_r = R(1.5\text{K})/R(300\text{K})$  with the diameter, as reported in the inset of Figure 2. The  $\rho_r$  ratio is found to be about 20 for the film, and it increases to about 30–40 for the biggest nanowires and jumps to 4000 for the 35-nm nanowires. An asymptotic behavior toward the film value is clearly observed for the larger diameters. This behavior indicates that an effect induced by the confined synthesis on the conjugated

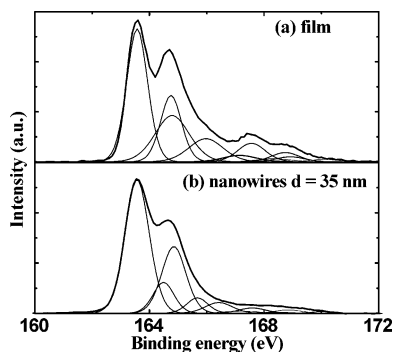


**Figure 3.** S(2p) signal from XPS spectra for (a) a PEDOT film and (b) 35-nm nanowires.

polymer conduction typically takes place for diameters smaller than 80 nm. To confirm this tendency, we also measured the temperature dependence of the resistance of nanowires synthesized under the same conditions but within pores of a commercial template, instead of UCL lab-scale membranes. These nanowires have a typical length of about 6  $\mu\text{m}$  and a real pore diameter distribution centered on 50 nm but with diameters ranging between 30 and 60 nm, as determined by SEM (pore diameter given by the manufacturer: 30 nm).<sup>22</sup> The  $\rho_r$  ratio of these nanowires is about 1300 as reported in the inset of Figure 2. The  $x$ -axis lateral size of the point reflects the diameter distribution measured by SEM. It confirms the tendency discussed previously, i.e., a sharp increase in the insulating character of PEDOT for the smaller diameters. It also indicates that the  $\rho_r$  variation does not depend on the type of polycarbonate membranes used as templates. These results are further analyzed in the Discussion.

**XPS Measurements.** Additional experiments are required to tentatively explain the results of our electrical study. We already reported on Raman spectroscopy studies to address modification of the electronic structure for PEDOT nanowires.<sup>17</sup> But the doping level of PEDOT nanowires was not yet determined. It has been shown that doping of PEDOT films prepared with the same aqueous solution as the one used in this work is due to a charge transfer from both  $\text{ClO}_4$  counterions and dodecyl sulfate anions from the surfactant.<sup>20</sup> X-ray photoelectron spectroscopy (XPS) analysis allows us to determine the doping level of PEDOT for two samples electropolymerized under the same conditions, a film and 35-nm nanowires. As shown in Figure 3, the S(2p) signal includes five components (each one is a doublet), three for the sulfur atoms of the EDOT chains and two for the sulfur atoms of the dodecyl sulfate anions. For the sulfur atoms of the EDOT chains, two doublets respectively at 163.6 and 164.8 eV (S1) and 164.8 and 166.0 eV (S2) are attributed to the EDOT sulfur atom in the neutral and the partially oxidized state.<sup>20</sup> A shake-up doublet at 167.1 and 168.3 eV (S3) is also introduced, as proposed by Tourillon et al.<sup>23</sup> For the sulfur atoms of the dodecyl sulfate (DS) anions, two doublets are identified respectively at 167.6 and 168.8 eV, and at 169.0 and 170.2 eV. These attributions are confirmed by XPS studies of a SDS powder (without PEDOT) and of a PEDOT film without SDS. Comparison between the S(2p) spectra for the film and for the 35-nm nanowires (Figure 3) clearly suggests that the doping level is reduced for the nanowires, as the bands for  $\text{DS}^-$  anions at higher energies are less pronounced. The doping level per EDOT monomer  $(I_{\text{DS}} + I_{\text{Cl}})/I_{\text{S\_EDOT}}$  in the samples is quantitatively determined from the atomic ratios  $I_{\text{DS}}$  of sulfur from DS anions and  $I_{\text{Cl}}$  of chlorine from  $\text{ClO}_4$  anions, with  $I_{\text{S\_EDOT}} = (I_{\text{S1}} + I_{\text{S2}} + I_{\text{S3}})$  being the total contribution of sulfur from EDOT chains. All fits for each band have a full

**TABLE 1: XPS Atomic Ratios of PEDOT for the Film and the 35-nm Nanowires<sup>a</sup>**

XPS atomic ratio	film	nanowires ( $d = 35$ nm)
$I_{\text{DS}}/I_{\text{S\_EDOT}}$	0.14	0.10
$I_{\text{Cl}}/I_{\text{S\_EDOT}}$	0.18	0.10
$(I_{\text{DS}} + I_{\text{Cl}})/I_{\text{S\_EDOT}}$	0.32	0.20
$I_{\text{S2}}/I_{\text{S\_EDOT}}$	0.34	0.17

<sup>a</sup> DS, Cl, S2, and S\_EDOT refer respectively to sulfur from DS anions, Cl from  $\text{ClO}_4$  anions, oxidized sulfur from PEDOT chains, and every sulfur contribution from PEDOT chains.

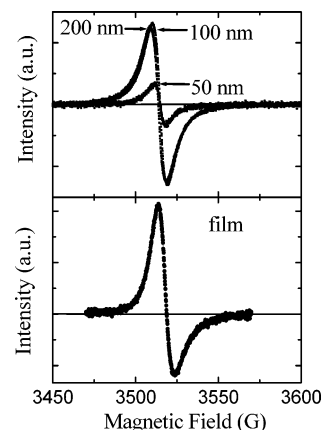


**Figure 4.** ESR spectra for 50-, 100-, and 200-nm nanowires (up) and a PEDOT film (down) at 9.4 GHz.

width at half-maximum smaller than 1.4 eV and the differences between fits and experimental data are about 1%. A doping level of 0.32/monomer is found for the film. It drops to 0.20/monomer for the 35-nm nanowires (see Table 1). The decrease in the doping level could be explained by a decrease in the doping species concentration within the pores due to a lower diffusion through nanometric dimensions. Remarkably, the doping level deduced from the atomic ratio of sulfur in the partially oxidized state  $I_{\text{S2}}/I_{\text{S\_EDOT}}$  gives similar values for the film (0.34/monomer) and the 35-nm nanowires (0.17/monomer), thus resulting in a drop of the doping level by a factor of 2. It also shows that most of the charge has been transferred on the heterocycle of the EDOT monomer. Such a reduction of the doping level influences the transport properties.

**ESR Study.** Additional information on the nature of the charge (polaronic, bipolaronic) carriers is required to explain the electrical behavior. ESR may give this information. For this study, we used commercial polycarbonate membranes as templates. Figure 4 compares room temperature spectra of PEDOT film and nanowires with real diameters approximately equal to 200, 100, and 50 nm (as measured by SEM) and normalized to the same EDOT mass. The film clearly has a Dysonian line shape, whereas the nanowires have symmetric Lorentzian shapes. The Dysonian shape is characteristic of a heavily doped polymer, which agrees with both XPS and transport results. It inhibits the intensity comparison between the film and the nanowires. For the nanowires, the Lorentzian peak area is directly proportional to the spin density. The comparison between the different areas shows thus that the spin density of the 200- and 100-nm nanowires is about 8 times larger than that for the 50-nm nanowires for which a spin density of  $8.5 \times 10^{-4}$  spin/EDOT is found. Assuming that the doping level for the larger diameters is close to the film case, that is about 2 times larger than for the smaller diameters, results in a decrease by at least a factor of 4 of the spin/charge ratio when the diameter decreases from 100 to 50 nm. Indeed, such a



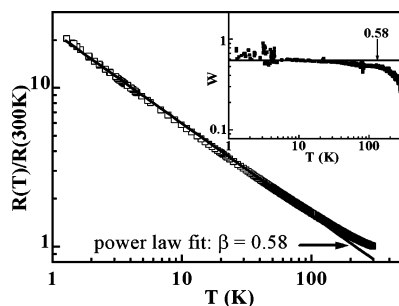


**Figure 5.** Temperature dependence of the resistance  $R(T)$  normalized by  $R(300\text{K})$  for a PEDOT film. The straight line corresponds to the ideal power law variation with an exponent of 0.58. Inset: Reduced activation energy  $W$  for the film versus the temperature.

decrease in the spin/charge ratio suggests a reduction of the polarons density to the benefit of the bipolarons one. Considering a doping level for the 50-nm nanowires close to 0.17/monomer as measured for the 35-nm nanowires, a rough estimation of the spin/charge ratio gives  $5 \times 10^{-3}$  spin/charge for the 50-nm nanowires. This very low spin/charge ratio (as well as the spin density) shows also that bipolarons are the dominant charge carriers in our nanowires, in agreement with results from Groenendaal and co-workers,<sup>24</sup> who have shown that bipolarons dominate for alkylated PEDOT in the range of doping concerned by our samples. Still, the variation by a factor of 4 of the spin/charge ratio with the nanowire diameter has to be explained. This point is discussed below in view of all the results.

## Discussion

In this work, we have found that the room temperature conductivity is roughly constant whatever the PEDOT nanowire diameter. But electrical measurements down to 1.5 K give evidence in strong reinforcement of the insulating character when the diameter decreases. The XPS study shows a doping level reduced by about a factor of 2 for 35-nm nanowires, in comparison with the film. The ESR study indicates a reduction by a factor of 4 of the polarons density to the benefit of the bipolarons when the nanowire diameter decreases.

Transport measurements on both film and nanowires can be further analyzed to identify the regime of conduction. The temperature dependence  $R(T)/R(300\text{K})$  of the PEDOT film is plotted in log–log scale in Figure 5. It shows that the resistivity follows a power law dependence with the temperature  $\rho(T) \propto T^{-\beta}$ . Such a dependence is characteristic of a conducting polymer close to the metal–insulator transition. The exponent  $\beta = 0.58$  is found, which effectively ranges between 0.33 and 1, as proposed by Larkin and Khmel'nitskii.<sup>25</sup> The values of the three parameters deduced from our experiments  $\sigma(300\text{K}) = 61 \text{ S}\cdot\text{cm}^{-1}$ ,  $\rho_r = 18$ ,  $\beta = 0.58$  suggest that the extent of disorder in PEDOT film is near the critical disorder for the metal–insulator transition. These results are in agreement with the work of Aleshin et al.,<sup>26</sup> who identify the critical regime of PEDOT for the following parameters:  $\sigma(300\text{K}) = 27 \text{ S}\cdot\text{cm}^{-1}$ ,  $\rho_r = 20$ ,  $\beta = 0.6$ . Further insight into the critical regime can be obtained in considering the reduced activation energy  $W(T)$  defined as:<sup>27</sup>

$$W(T) = -d(\ln\rho(T))/d(\ln T)$$

The negative slope of  $W(T)$  in log–log scale for the film (inset of Figure 5), i.e., the decrease of  $W$  with increasing temperature, implies that the PEDOT film is on the insulating side of the M–I transition.

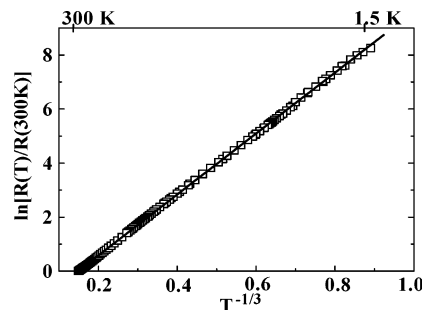


**Figure 6.** Temperature dependence of the resistance  $R(T)$  normalized by  $R(300\text{K})$  for 35-nm nanowires. The straight line corresponds to the fit with the Mott-VRH 2D model.

As already pointed out, the weak temperature dependence of the film resistivity contrasts with the strong one for the 35-nm nanowires. Actually, the temperature dependence of the resistivity cannot be described with a power law. Instead, the resistance of the 35-nm nanowires varies as  $\ln(R(T)/R(300\text{K})) \propto T^{-1/3}$ , as shown in Figure 6. This behavior suggests that transport occurs by Mott-Variable Range Hopping (VRH)<sup>28</sup> for which  $R(T) = R_0 \exp(T_0/T)^{1/(1+d)}$ , with  $d$  being the dimension of the conduction path, equal to 2. An excellent agreement between the fit and the experiment is obtained over the whole temperature range 1.5–300 K for  $T_0 \approx 1400 \text{ K}$ . Kuzmany et al.<sup>29</sup> showed  $T_0$  versus  $\sigma(300\text{K})$  plots along a universal curve for numerous conjugated polymers. From this universal plot, the room temperature conductivity corresponding to  $T_0 = 1400 \text{ K}$  is equal to  $30\text{--}60 \text{ S}\cdot\text{cm}^{-1}$ , in very good agreement with  $\sigma(300\text{K})$  estimated for our nanowires.

The appearance of a 2D conduction mechanism in our nanowires deserves a comment. A similar mechanism has been observed in PPY and PANI nanotubes. For these systems, Spatz et al.<sup>30</sup> schematized the template-prepared nanotubes by a surface layer of highly ordered polymer chains and an inner layer of disordered material on the basis of many studies such as IR and Raman spectroscopies, PIRAS (polarized IR absorption spectroscopy), and XRD studies.<sup>5–8</sup> They observed a crossover from a 3D Mott-VRH conduction for 200-nm nanotubes to a 2D Mott-VRH conduction for 50-nm nanotubes. They attribute this crossover to a charge-carrier hopping distance larger than either the nanotube wall thickness or the thickness of the highly ordered surface layer for the small diameters. Indeed, they were not able to make any conclusions because the two thicknesses decrease with the nanotube diameter. We suggest here to adopt a similar sketch for the smaller PEDOT nanowires, i.e., the 2D conduction mechanism originates from a heterogeneous structure of the nanowire with a conducting surface layer and a more insulating inner core. The existence of an ordered layer can be supported by our structural investigations. It is now clear that there is an improvement of the molecular and the supermolecular structure for the smaller PEDOT nanowires, as suggested by Raman and absorption spectroscopy studies.<sup>17</sup> Such an enhanced ordering could also explain the reduction of the polarons density to the benefit of the bipolarons when the nanowire diameter decreases, as deduced from the ESR study in this work. This improvement of the structure is indeed related to the growth mechanism and it is likely confined to the interface between the pore and the wire. It is thus expected for the smaller PEDOT nanowires (35-nm diameter) that the conduction takes place predominantly within the pretty well ordered surface layer. Thus, such a heterogeneous structure of the nanowire could explain the 2D conduction mechanism of the smaller PEDOT nanowires when the hopping distance is larger than the ordered surface layer thickness.

Whereas two regimes of conduction are clearly identified for the 35-nm nanowires and for the film, variations of the resistance with the temperature for the 75- and 150-nm nanowires present an intermediate behavior that can be analyzed neither by one of these two regimes nor by ES-VRH and any Mott-VRH model. We also considered the case of an inhomogeneous material but Sheng's model<sup>31</sup> cannot account for the variation measured for the large diameter nanowires as well. Finally, a model based on a conduction by two independent channels in parallel has been developed: one channel conducts electrically like the film whereas the other channel conducts like the 35-nm nanowires. This model failed to fit the variations for the 75- and 150-nm nanowires, whatever the proportion of each channel. Such a result supports the fact that the scheme introduced by Martin and co-workers is oversimplified for the larger diameters. As the doping level is modified by the confined synthesis, an inhomogeneous doping may also take place through the nanowire for the larger diameters.

Additional information about the ordered layer can be deduced from the discussion of the following paradox: on one hand, a roughly constant room temperature conductivity whatever the nanowire diameter and, on the other hand, a reinforcement of the insulating character when the diameter decreases as evidenced by the  $R(T)$  variations. This apparent contradiction can only be explained if competitive effects are involved. For the smaller diameter nanowires, we have already discussed the improved ordering and the increase in bipolarons density (as deduced from Raman, absorption, and ESR spectroscopy studies) which should improve the conductivity. This is partly balanced by the decrease in the doping level. Indeed, it is reasonable for conjugated polymers to consider that a doping level divided by about a factor of 2 affects the charge density quantitatively in a similar way. So, it can explain why the insulating character is more pronounced for the nanowires, since the metal–insulator transition is reached only for heavily doped conjugated polymers. But it can definitely not explain the strong variation of the resistance ratio  $\rho_r$ , which is 200 times larger for the 35-nm nanowires than for the film. This last point is still unclear. We suggest that, because of the template synthesis, the polymer chains of the ordered outer layer align preferentially perpendicular to the wire axis, i.e., perpendicular to the current in our geometry of measurement, as previously evidenced by Menon et al.<sup>7</sup> Such an ordered layer should control the conduction within the smaller nanowires. It will require for a charge a much larger number of hopping events in order to cross the nanowire from bottom to top than if the polymer chains were randomly distributed and thus it will result in a larger  $\rho_r$  ratio. At room temperature, however, the different effects may compensate to let the conductivity be nearly unchanged whatever the diameter.

## Conclusion

In contrast with PPY and PANI nanotubes, the estimated room temperature conductivity for PEDOT nanowires is only weakly affected by the nanowire diameter. Transport measurements down to 1.5 K are performed for PEDOT nanowires and film. Surprisingly, a reinforcement of the insulating character when the diameter decreases is evidenced. The analysis of the resistance variation with the temperature shows that our samples range between two tendencies: a 2D Mott-variable range hopping in the 35-nm nanowires and a film close to the metal–insulator transition. A structural improvement and an increase in the conjugation length for the smaller diameters, as already reported on various conjugated polymers nanowires, may result

in the opposite behavior. Our results clearly indicate that a competitive effect induced by the confined synthesis is involved. The doping level has been addressed by XPS. The significantly smaller doping level for the 35-nm nanowires than for the film gives evidence that the doping level plays an important role but it cannot account for the whole effect. This study indicates that, besides the improvement of the molecular and the supermolecular structure, the confined synthesis within nanopores of a template can generate a broad variety of electrical behavior for conjugated polymers.

**Acknowledgment.** We thank Dr. S. Demoustier-Champagne for providing us with polycarbonate membranes fabricated at the Université Catholique de Louvain (Belgium). J.L.D. gratefully acknowledges A. Barreau for his help with FE-SEM studies.

## References and Notes

- (1) Koopal, C. G. J.; Feiters, M. C.; Nolte, R. J. M.; de Ruiter, B.; Schasfoort, R. B. M.; Czajka, R.; Van Kempen, H. *Synth. Met.* **1992**, *51*, 397. Kuwabata, S.; Martin, C. R. *Anal. Chem.* **1994**, *66*, 2757.
- (2) Kim, B. H.; Kim, M. S.; Park, K. T.; Lee, J. K.; Park, D. H.; Joo, J.; Yu, S. G.; Lee, S. H. *Appl. Phys. Lett.* **2003**, *83*, 539.
- (3) Saha, S. K. *Appl. Phys. Lett.* **2002**, *81*, 3645.
- (4) Granström, M.; Berggren, M.; Inganäs, O. *Science* **1995**, *267*, 1479.
- (5) Martin, C. R. *Science* **1994**, *266*, 1961.
- (6) Martin, C. R. *Handbook of Conducting Polymers*, 2nd ed.; Skotheim, T. A., Elsenbaumer, R. L., Reynolds, J. R., Eds.; Marcel Dekker: New York, 1998; p 409 and references therein.
- (7) Menon, V. P.; Lei, J.; Martin, C. R. *Chem. Mater.* **1996**, *8*, 2382.
- (8) Cai, Z.; Lei, J.; Liang, W.; Menon, V.; Martin, C. R. *Chem. Mater.* **1991**, *3*, 960.
- (9) Demoustier-Champagne, S.; Stavaux, P. Y. *Chem. Mater.* **1999**, *11*, 829.
- (10) Granström, M.; Carlberg, J. C.; Inganäs, O. *Polymer* **1995**, *36*, 3191.
- (11) Duchet, J.; Legras, R.; Demoustier-Champagne, S. *Synth. Met.* **1998**, *98*, 113.
- (12) de Jong, M. P.; van Ijzendoorn, L. J.; de Voigt, M. J. A. *Appl. Phys. Lett.* **2000**, *77*, 2255.
- (13) Möller, S.; Perlov, C.; Jackson, W.; Taussig, C.; Forrest, S. *Nature* **2003**, *426*, 166.
- (14) Groenendaal, L.; Jonas, F.; Freitag, D.; Pielartzik, H.; Reynolds, J. R. *Adv. Mater.* **2000**, *12*, 481.
- (15) Granström, M.; Inganäs, O. *Polymer* **1995**, *36*, 2867.
- (16) Joo, J.; Park, K. T.; Kim, B. H.; Lee, S. Y.; Jeong, C. K.; Lee, J. K.; Park, D. H.; Yi, W. K.; Lee, S. H.; Ryu, K. S. *Synth. Met.* **2003**, *135*, 7.
- (17) Duvail, J. L.; Rétho, P.; Garreau, S.; Louarn, G.; Godon, C.; Demoustier-Champagne, S. *Synth. Met.* **2002**, *131*, 123. Buisson, J. P.; Rétho, P.; Louarn, G.; Duvail, J. L. To be submitted for publication.
- (18) Hanot, H.; Ferain, E.; Legras, R. Patent WO0149403, 2001. Ferain, E.; Legras, R. *Nucl. Instrum. Methods B* **1994**, *84*, 331.
- (19) Sakmeche, N.; Aaron, J.-J.; Fall, M.; Aeiyaeh, S.; Jouini, M.; Lacroix, J.-C.; Lacaze, P.-C. *Chem. Commun.* **1996**, 2723.
- (20) Sakmeche, N.; Aeiyaeh, S.; Aaron, J.-J.; Jouini, M.; Lacroix, J.-C.; Lacaze, P.-C. *Langmuir* **1999**, *15*, 2566.
- (21) Mativetsky, J. M.; Datars, W. R. *Physica B* **2002**, *324*, 191.
- (22) Schönenberger, C.; van der Zande, B. M. I.; Fokkink, L. G. J.; Henny, M.; Schmid, C.; Krüger, M.; Bachtold, A.; Huber, R.; Birk, H.; Stauffer, U. *J. Phys. Chem. B* **1997**, *101*, 5497.
- (23) Tourillon, G.; Jugnet, Y. *J. Chem. Phys.* **1988**, *89*, 1905.
- (24) Groenendaal, L.; Zotti, G.; Jonas, F. *Synth. Met.* **2001**, *118*, 105.
- (25) Larkin, A. I.; Khmel'nitskii, D. E. *Sov. Phys. JETP* **1982**, *56*, 647.
- (26) Aleshin, A.; Kiebooms, R.; Menon, R.; Heeger, A. J. *Synth. Met.* **1997**, *90*, 61.
- (27) Zabrodskii, A. G.; Zinov'eva, K. N. *Sov. Phys. JETP* **1984**, *59*, 425.
- (28) Mott, N. F.; Davis, E. A. *Electronic Processes in Non-crystalline Materials*; Clarendon Press: Oxford, UK, 1979.
- (29) Kuzmany, H.; Mehring, M.; Roth, S. *Springer Ser. Solid-State Sci.* **1987**, *76*, 38.
- (30) Spatz, J. P.; Lorenz, B.; Weishaupt, K.; Hochheimer, H. D.; Menon, V.; Parthasarathy, R.; Martin, C. R.; Bechtold, J.; Hor, P. H. *Phys. Rev. B* **1994**, *50*, 14888. See also: Orgzall, I.; Lorenz, B.; Ting, S. T.; Hor, P. H.; Menon, V.; Martin, C. R.; Hochheimer, H. D. *Phys. Rev. B* **1996**, *54*, 16654. Mikat, J.; Orgzall, I.; Lorenz, B.; Sapp, S.; Martin, C. R.; Burris, J. L.; Hochheimer, H. D. *Physica B* **1999**, *265*, 154.
- (31) Sheng, P.; Abeles, B.; Arie, Y. *Phys. Rev. Lett.* **1973**, *31*, 44.